

# Trapping Ultracold Atoms in a Time-Averaged Adiabatic Potential

M. G. Kildemister, E. Nugent, B. E. Sherlock, M. K. Kubasik, B. T. Sheard, and C. J. Foot  
 Clarendon Laboratory, University of Oxford, Parks Road, Oxford, OX1 3PU, United Kingdom  
 (dated: February 22, 2024)

We report the first experimental realization of ultracold atoms confined in a time-averaged, adiabatic potential (TAAP). This novel trapping technique involves using a slowly oscillating (kHz) bias field to time-average the instantaneous potential given by dressing a bare magnetic potential with a high frequency (MHz) magnetic field. The resultant potentials provide a convenient route to a variety of trapping geometries with tunable parameters. We demonstrate the TAAP trap in a standard time-averaged orbiting potential trap with additional Helmholtz coils for the introduction of the radio frequency dressing field. We have evaporatively cooled  $5 \times 10^4$  atoms of  $^{87}\text{Rb}$  to quantum degeneracy and observed condensate lifetimes of over 3 s.

PACS numbers: 37.10.Gh, 32.80.Xx, 03.75.-b

The use of increasingly sophisticated magnetic potentials has been crucial to the evolution of cold atom research. The time-averaged adiabatic potential (TAAP) trap proposed in [1] combines the techniques of time-averaging and radio frequency (RF) dressing to produce versatile potentials with a rich variety of different geometries. Since the RF dressing only couples electronic ground states of the atom the rate of relaxation by spontaneous processes is negligible. The potential is smooth with no small scale corrugations because the trapping region is located far from the field generating coils. As shown in [1], the TAAP can easily sculpt complex trapping geometries such as a double-well or ring trap, which can be adiabatically modified. Here we present an experimental realization of the particular case of a double-well TAAP and an efficient way of loading it from a time-orbiting potential (TOP) trap.

The technique of time-averaging involves the introduction of a time dependence to a static potential at a frequency higher than the atoms can respond to kinematically, but significantly lower than the local Larmor frequency. As a result atoms experience a modified potential whilst preserving their initial  $m_F$  state. The application of a suitable rotating bias field to a quadrupole potential can circumvent Majorana losses by ensuring the field zero orbits at a radius greater than the extent of the atom cloud. For a bias field  $B_T$  rotating at angular frequency  $\omega_T$  the criterion for time-averaging can be stated as  $\hbar \omega_T B_T \gg \hbar \omega_T > \hbar \omega_r$ , where  $g_F$  is the Landé g-factor,  $\mu_B$  the Bohr magneton,  $\hbar$  the reduced Planck constant and  $\omega_r$  the oscillation frequency of atoms in the time-averaged potential. This time-averaged, orbiting potential not only expedited the first realization of a Bose-Einstein Condensate (BEC) in a dilute alkali vapor [2], but also paved the way for more sophisticated magnetic potentials such as a double-well [3] and ring-shaped potentials [4-6]. The general concept of using time-averaging to create novel shapes of confining potentials has also been demonstrated by experiments on dipole force traps [7-9].

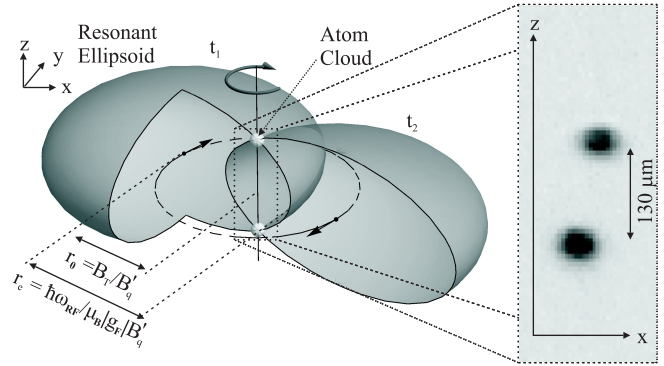


FIG. 1. The instantaneous potential of the TAAP trap at two different times in the rotation cycle. The intersection of this potential with the rotation axis gives the minimum of the TAAP at which the AP remains stationary. The inset shows an in-situ absorption image of a thermal cloud trapped at these positions. We attribute the tilt evident in this image to a misalignment of the rotation axis with respect to the symmetry axis of the quadrupole potential.

The repertoire of magnetic potentials was further extended by RF dressing, as proposed by Zobay and Garraway [10]. Their technique brought about the possibility of highly asymmetric 2D magnetic potentials [11-13]. It has also been applied in atom chip experiments to give flexible double-well potentials [14, 15] as described in detail elsewhere [10, 16-18]. RF dressing involves a magnetic field oscillating at a frequency  $\omega_{RF}$  comparable to the atomic Larmor frequency which drives transitions between Zeeman sub-levels in a hyperfine manifold of the atom's electronic ground state. Here the eigenstates of the system are the dressed states [19]. The variation of the corresponding eigenenergies with position gives rise to an adiabatic potential (AP) given by

$$U_{AP}(r) = m_F \hbar \omega_{RF} \frac{1}{\sqrt{1 + \frac{\omega_{RF}^2}{\omega_L^2}}} + \frac{1}{2} \mu_B B_T(r); \quad (1)$$

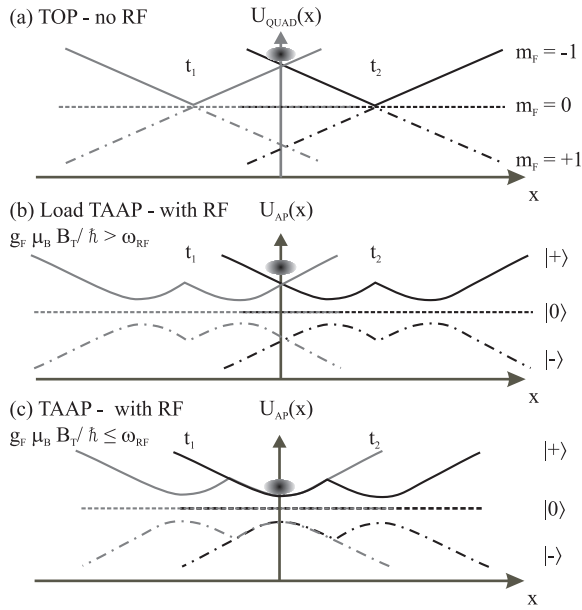


FIG. 2. The instantaneous potential of the (a) TOP, (b) TAAP loading and (c) TAAP potentials along the  $x$  axis at time  $t_1$  in the rotation cycle and time  $t_2$  half a period later.

where  $\delta(x) = \gamma_F B_T B(x) - \gamma$  is the angular frequency detuning and  $\Omega_R(x)$  the Rabi frequency given by

$$\Omega_R(x) = \gamma \frac{g_F \mu_B B(x)}{2\hbar} \frac{B(x)}{B_T} \quad (2)$$

In this experiment we use a quadrupole field of the form

$$B_q(x) = B_q^0 [x\hat{e}_x + y\hat{e}_y - 2z\hat{e}_z]; \quad (3)$$

where  $B_q^0$  is the radial gradient. When dressed with an RF field  $B_{RF}$  the upper dressed state has a minimum on an ellipsoidal iso- $B$  surface where  $\delta(x) = 0$ . The vectorial nature of the coupling (see Eq. 2) gives a variation of the potential on the ellipsoidal shell itself: for linearly polarized RF with  $B_{RF}(t) = B_{RF} \cos(\Omega_{RF} t)\hat{e}_z$  the coupling varies from maximum on the equator to zero at the poles. For circularly polarized RF with  $B_{RF}(t) = B_{RF} [\cos(\Omega_{RF} t)\hat{e}_x - \sin(\Omega_{RF} t)\hat{e}_y]$  the coupling is maximum at one pole and zero on the other [20].

RF dressed-state adiabatic potentials may themselves be time-averaged to give a new class of potentials referred to as time-averaged adiabatic potentials. We have generated a double-well TAAP by applying RF radiation to a conventional TOP trap. The instantaneous potential of the TOP is a quadrupole field, in a TAAP trap this is dressed to give the ellipsoidal surface as described above. The oscillating bias field of the TOP trap,  $B_T(t) = B_T [\cos(\Omega_T t)\hat{e}_x + \sin(\Omega_T t)\hat{e}_y]$ , causes the ellipsoidal surface to orbit in the  $xy$ -plane about the axis of rotation as

illustrated in Fig. 1. When  $\Omega_{RF} > \gamma_F B_T \approx \gamma$  the ellipsoidal surface intersects the rotation axis at two points; these two points define the minima of the time-averaged potential.

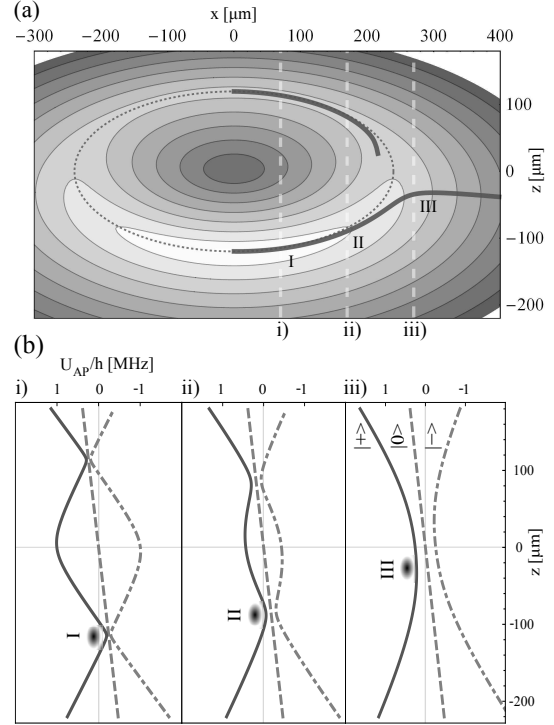


FIG. 3. (a) A contour plot of the AP in the  $xz$ -plane for a gradient of  $B_q^0 = 84 \text{ G/cm}$  and for linearly polarized RF with  $B_{RF} = 0.5 \text{ G}$ . The dashed lines indicate the position of the rotation axis of the ellipsoid for different values of  $B_T$ . (b) Shows the potential along these lines for the three dressed states. The slope in the potentials corresponds to the gravitational potential energy of a  $^{87}\text{Rb}$  atom. Note the variation of the coupling at the atom's position.

We load atoms into the double-well TAAP from a TOP using the following procedure. First, we prepare a sample of cold atoms in the TOP trap (see Fig. 2 (a)). The RF dressing field is then rapidly switched on while ensuring  $B_T$  satisfies the inequality  $\Omega_{RF} < \gamma_F B_T \approx \gamma < 2\Omega_{RF}$  (Fig. 2 (b)). The lower bound ensures the atoms are loaded into the correct dressed state while the upper bound is to prevent higher harmonics of  $\Omega_{RF}$  coming into resonance and causing unwanted evaporation. At this stage the modification of the time-averaged potential is minimal (the ellipsoids of Fig. 1 do not yet intersect with the rotation axis). Decreasing the TOP field to  $\Omega_{RF} = \gamma_F B_T \approx \gamma$  transfers the atoms onto the ellipsoidal shell (Fig. 2 (c)). A further decrease in the TOP field gives rise to a double-well potential in the  $z$  direction. Note that the atoms stay on resonance at all times in the TAAP trap. The well separation is given by the

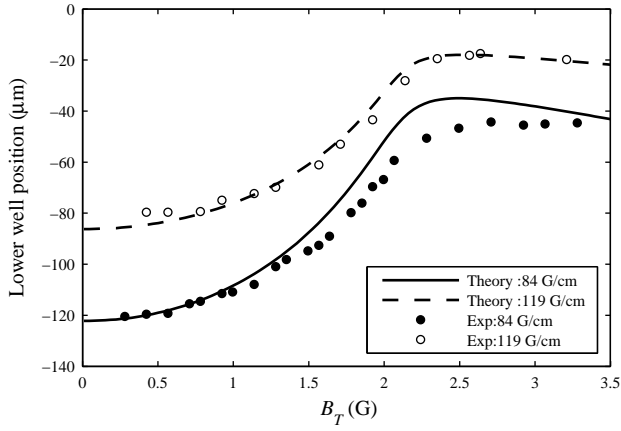


FIG. 4. Vertical displacement of the atoms from the static quadrupole field centre in the lower well of the TAAP trap as a function of the magnitude of the rotating bias field  $B_T$ . This is plotted for two different field gradients  $B_q^0 = 84 \text{ G/cm}$  and  $B_q^0 = 119 \text{ G/cm}$ .

distance between the points of intersection of the ellipsoidal surface with the rotation axis: a decrease in  $B_T$  moves the atom clouds further along the ellipsoid thus increasing their separation. The TAAP potential in the  $z$  direction is that along the rotation axis of the ellipsoid as depicted in Fig. 3. The effect of the time-averaging is to give confinement along the surface thus preventing the atoms spreading out over the ellipsoid.

Our TOP trap (with  $\nu_T = 2.7 \text{ kHz}$ ) apparatus routinely produces BEC's of  $1 \cdot 10^6$  atoms of  $^{87}\text{Rb}$  in the  $F = 1; m_F = -1$  hyperfine state. The RF dressing field is applied through coaxial coil pairs placed symmetrically about the trap center along the  $x; y$  and  $z$  axes; this allows any arbitrary polarization but in these experiments it was either polarized circularly with  $B_{\text{RF}}(t)$  in the  $xy$ -plane or linearly with  $B_{\text{RF}}(t) / \hat{e}_z$ .

In Fig. 4 the vertical position of atoms in the lower well of the TAAP trap is plotted as a function of the magnitude of the rotating bias field  $B_T$  for two different quadrupole gradients. Here we apply linearly polarized RF along the  $z$  direction with  $B_{\text{RF}} = 0.5 \text{ G}$  and  $\nu_{\text{RF}} = 2.14 \text{ MHz}$ . For these parameters the ellipsoidal surface touches the rotation axis when  $B_T = 2 \text{ G}$  at which stage the atoms are loaded into the TAAP trap. The polarization effects mentioned above and the gravitational sag of the atoms mean that as  $B_T$  is lowered the atoms do not follow the perfect ellipsoidal trajectory that one would expect from the idealized picture above (in Fig. 3 compare the dotted ellipsoid to the actual position of the minimum shown in black).

It is evident in Fig. 3 that gravitational sag makes it impossible to load into the upper well for this quadrupole

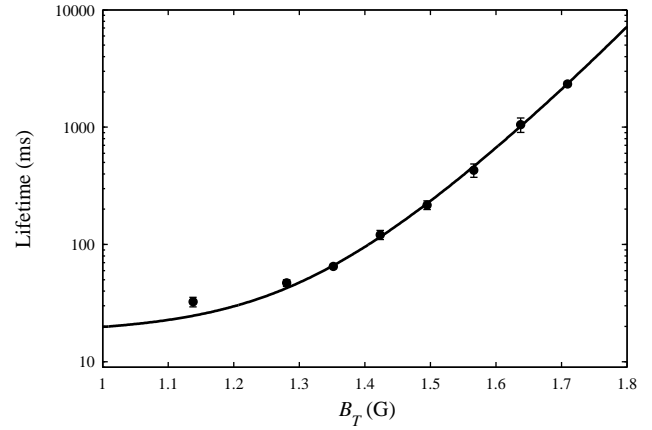


FIG. 5. The lifetime of atoms in the TAAP trap for linearly polarized RF with  $B_{\text{RF}} = 0.5 \text{ G}$  and a radial quadrupole gradient of  $B_q^0 = 84 \text{ G/cm}$ . For this polarization of RF the  $\nu_{\text{R}}(r)$  varies linearly with  $B_T$  (see text for more details).

gradient (as denoted by the discontinuity in the black line in Fig. 3 indicating positions where there is no minimum in the upper half of the potential). This difficulty can be overcome by loading at higher gradients ( $230 \text{ G/cm}$ ) and lowering  $B_T$  to a final value of  $1.7 \text{ G}$ . A subsequent decrease in the gradient over  $400 \text{ ms}$  (limited by speed of power supply) to  $80 \text{ G/cm}$  fully splits the cloud (see absorption image of Fig. 1). Using higher values for  $B_T$  during this loading procedure decreases the barrier height and prevents atoms from staying in the upper well. Lower values for  $B_T$  decrease the coupling at the potential minimum and result in an insufficient lifetime to observe the separated clouds. The chosen values balance these competing effects.

In addition the reduced lifetime explains why no data was taken in Fig. 4 for  $B_T < 0.4 \text{ G}$  as the lifetime proved to be insufficient to make reliable measurements of the position. This effect is due to Landau-Zener (LZ) transitions to untrapped dressed states. The LZ transition probability for transitions between adjacent dressed states in the  $F = 1$  manifold is given by [21]

$$P_{\text{LZ}}(r) = 1 - \exp\left[-\frac{\nu_{\text{R}}^2(r)}{2g_{\text{FB}}^2 B_q^0 v}\right]; \quad (4)$$

where  $v$  is the velocity of the atom through the avoided crossing. The lifetime of atoms in the TAAP trap varies as  $\tau = \tau_0 / P_{\text{LZ}}(r)$  where the offset  $\tau_0$  takes into account the finite extent of the cloud. Fig. 5 shows the variation in trap lifetime for a TAAP dressed with linearly polarized RF. For this polarization  $\nu_{\text{R}}(r)$  is a linear function of  $B_T$  and the lifetime changes by two orders of magnitude as  $B_T$  is ramped down. By choosing circularly polarized RF of the appropriate handedness one can

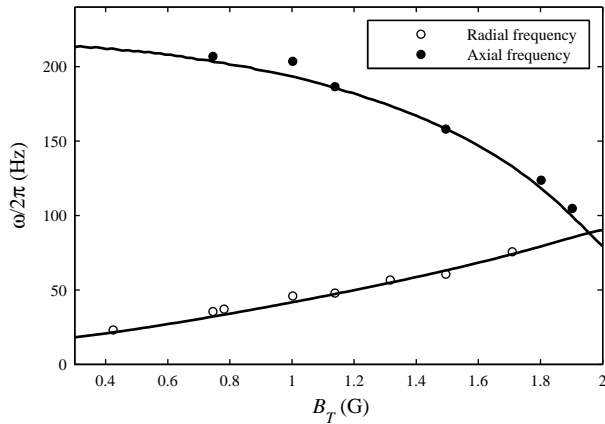


FIG. 6. Trapping frequencies of the atoms in the lower well of the TAAP trap as a function of the magnitude of the rotating field  $B_T$ . These frequencies are for a TAAP dressed with circularly polarized RF,  $B_{RF} = 0.5$  G, and for  $B_q^0 = 84$  G/cm.

engineer a situation where the Rabi frequency increases as  $B_T$  is lowered. In this case we apply RF fields in two directions each with an amplitude of  $B_{RF} = 0.5$  G. The predicted Rabi frequency  $\sim 300$  kHz close to the south pole of the ellipsoidal surface agrees well with spectroscopy measurements of the trap bottom. These effects combine to give a lifetime of up to 10 s in the lower TAAP well. In addition, we have measured trapping frequencies as a function of  $B_T$  and observed good agreement with theoretical predictions as shown in Fig. 6. In this trap we have successfully cooled a thermal cloud to quantum degeneracy. Starting with a sample of  $1.5 \times 10^6$  atoms at 0.7 K in the TOP trap, we observe an atom loss of approximately a third during the TAAP loading process with no substantial heating. The loss mechanism is attributed to increased Landau-Zener losses when the avoided crossing spirals through the cloud. A subsequent rf-evaporation sweep over 3 s with an additional weaker field (0.05 G) cools the sample below the critical temperature creating a BEC of  $5 \times 10^4$  atoms. For these frequency sweeps we have used transitions both within and beyond the rotating-wave approximation (RWA) and observed comparable efficiencies [16]. A BEC can be held in the TAAP trap without any evaporative rf for more than 3 s without any discernible heating.

In conclusion we have presented the first realization of a time-averaged adiabatic potential which promises an accessible route to a large variety of purely magnetic trapping geometries with tunable parameters. The loading scheme presented above has acceptable losses and

negligible heating. Furthermore, we show it is possible to evaporatively cool atoms to below quantum degeneracy in such a potential. Since completing the work presented above, we have successfully employed the TAAP trap as an intermediate stage for loading a radio frequency dressed-state potential (lowering  $B_T$  to zero) which is of interest for studying of low dimensional physics [10].

This work has been supported by the EPSRC under grant EP/D000440.

- 
- [1] I. Lesanovsky and W. von Klitzing, *Phys. Rev. Lett.* **99**, 083001 (2007).
  - [2] M. H. Anderson, J. R. Ensher, M. R. Matthews, C. E. Wieman, and E. A. Cornell, *Science* **269**, 198 (1995).
  - [3] N. R. Thomas, A. C. Wilson, and C. J. Foot, *Phys. Rev. A* **65**, 063406 (2002).
  - [4] A. S. A. Mold, C. S. Garvie, and E. Riis, *Phys. Rev. A* **73**, 041606 (2006).
  - [5] P. F. Griffin, E. Riis, and A. S. A. Mold, *Phys. Rev. A* **77**, 051402 (2008).
  - [6] S. Gupta, K. W. Murch, K. L. Moore, T. P. Purdy, and D. M. Stamper-Kurn, *Phys. Rev. Lett.* **95**, 143201 (2005).
  - [7] P. Rudy, R. Ejnisman, A. Rahman, S. Lee, and N. Bigelow, *Opt. Express* **8**, 159 (2001).
  - [8] N. Friedman, L. Khaykovich, R. Ozeri, and N. Davidson, *Phys. Rev. A* **61**, 031403 (2000).
  - [9] K. Henderson, C. Ryu, C. M. McCormick, and M. G. Boshier, *New J. Phys.* **11**, 043030 (2009).
  - [10] O. Zobay and B. M. Garraway, *Phys. Rev. Lett.* **86**, 1195 (2001).
  - [11] Y. Colombe, E. Knjazhyan, O. Morozov, B. Mercier, V. Lorent, and H. Perrin, *Europhys. Lett.* **67**, 593 (2004).
  - [12] M. White, H. Gao, M. Pasienski, and B. Demarco, *Phys. Rev. A* **74**, 023616 (2006).
  - [13] O. Morozov, C. L. G. A. Lazar, P. E. Pottie, V. Lorent, and H. Perrin, *J. Phys. B* **40**, 4013 (2007).
  - [14] T. Schumm, S. Hoerberth, L. M. Andersson, S. Wildemuth, S. G. Roth, I. Bar-Joseph, J. Schmiedmayer, and P. Krüger, *Nat. Phys.* **1**, 57 (2005).
  - [15] S. Hoerberth, I. Lesanovsky, B. Fischer, J. Verdu, and J. Schmiedmayer, *Nat. Phys.* **2**, 710 (2006).
  - [16] S. Hoerberth, B. Fischer, T. Schumm, J. Schmiedmayer, and I. Lesanovsky, *Phys. Rev. A* **76**, 013401 (2007).
  - [17] I. Lesanovsky, T. Schumm, S. Hoerberth, L. M. Andersson, P. Krüger, and J. Schmiedmayer, *Phys. Rev. A* **73**, 033619 (2006).
  - [18] I. Lesanovsky, S. Hoerberth, J. Schmiedmayer, and P. Schmelcher, *Phys. Rev. A* **74**, 033619 (2006).
  - [19] C. Cohen-Tannoudji, J. Dupont-Roc, and G. Grynberg, *Atom-Photon Interactions* (Wiley, 1992).
  - [20] In making the rotating wave approximation the time-dependence of the Rabi frequency is removed.
  - [21] N. V. Vitanov and K. A. Suominen, *Phys. Rev. A* **56**, R4377 (1997).